Geometric Modeling of 3D-Face Features and Its Applications

Vandana D. Kaushik
Department of Computer Science and Engineering,
Harcourt Butler Technological Institute,
Kanpur 208 002, India
vandanadixitk@yahoo.com

V. K. Pathak
Department of Computer Science and Engineering,
Harcourt Butler Technological Institute,
Kanpur 208 002, India
vinaypathak.hbti@gmail.com

P. Gupta
Department of Computer Science and Engineering,
Indian Institute of Technology Kanpur,
Kanpur208 016, India
pg@cse.iitk.ac.in

***Abstract*— This paper proposes a method of geometric modeling of features extracted from 3D face and presents some of its applications. It describes a new automatic pose and expression invariant feature extraction algorithms to extract features (control points) from eyebrows, nose and lips of 3D facial data. The proposed algorithms are tested on BU-3DFE (Binghamton University 3D Facial Expression) Database where each subject has at least six expressions. Three dimensional curves are fitted on these extracted features. Through Chi-Square test it reveals that the curve fitted against each extracted feature is found to be good with 98.5% confidence level. In this paper, the proposed geometric model has been used in 3D face recognition and in regeneration of all features. It has been found that the model helps to reduce the storage space considerably and can be used as a soft biometric tool to classify the biometric images in the database so that search space in the database for identification can be reduced substantially.**

***Index Terms*—3D Face Recognition, Geometric Modeling, Feature Extraction, Regeneration, Pose and Expression Invariant**

I. Introduction

Feature extraction from the 3D face is one of the primary tasks in a face recognition system. Generally any feature of a given 3D face consists of huge volume of data points. As a result, it becomes difficult to store all features in the large database. Further, a face recognition system recognizes a person by matching facial feature characteristics (vectors) possessed by that person. A naïve identification system compares the given feature vectors in the database. For a large database containing 3D facial feature vectors, it may require a long response time for identification which may not be desirable. A feature based classification technique can be used to reduce the search space in the database. This paper proposes an efficient method to model these 3D features geometrically so that it not only addresses the above said issues but also can be used to regenerate the 3D face from the derived geometric models.

Feature extraction algorithm proposed by Zhao et. al. [27] has selected the feature points manually from a given face and therefore, this algorithm is dependent on user accuracy. There exists a number of automatic feature extraction algorithms which are based on Gabor Wavelet Transform [5], Eigenvectors [12] and Fisher Linear Discriminant Analysis [3] etc. These algorithms work generally under controlled environment with respect to lighting conditions and stable frontal view images of faces.

Some of the well known statistical based 2D facial feature extraction algorithms are Independent Component Analysis [ICA] [2], Linear Discriminant Analysis [LDA] [3] and Principal Component Analysis [PCA] [12]. These algorithms try to extract facial features from the whole face. PCA based algorithms are popular because of the ease of implementing them and their reasonable performance levels [18] [21]. However, overall performance of these algorithms mainly depends on the quality and type of the images being processed. Further, most of these algorithms are sensitive to pose, illumination and expression of the image. Thus, there is a need to design face recognition algorithm which is invariant to the above mentioned factors. Efforts have been made to handle some of these factors by considering 3D faces [7], [22], [27]. Recently, PCA based techniques have also been applied to 3D face data [9][20]. A PCA based technique with embedded hidden Markov models on 3D faces has been proposed by Tsalakanidou et. al. [25]. Along with PCA, LDA [8] and ICA [24] have also been used for the analysis of 3D data. All these statistical methods including 3D do not consider the effects of facial expressions and very large variations in pose. Automatic feature extraction algorithm from 2.5D scans has been proposed by Lu and Jain in [14]. This can handle pose invariance efficiently.

Surface-based algorithms form another class of algorithms which can be used to extract features from 3D face. These algorithms are either based on Local Methods [19] or Global Methods [11], [23]. In [26] a hybrid

doi:10.4304/jcp.5.9.1305-1314

algorithm that uses both local and global geometric surface information has been proposed. But point sets or profiles used in these algorithms are found to be difficult to define.

The statistical methods and most of the surfaced based methods for face recognition do not deal with effect of facial expressions. Even though effect of expressions is handled in [4] but only two such variations are considered. There are number of model-based approaches for face recognition which are fairly insensitive to viewpoint [13]. One of these approaches is based on 3D deformable modeling [15] which can simultaneously handle both pose and expression variations. However, these approaches are computationally expensive and sensitive to initialization.

This paper proposes new algorithms for feature extraction from a 3D face. These algorithms are invariant to pose and illumination and can be used for automatic extraction of facial feature regions like eyebrows, nose and lips from a 3D face. Control points (termed as features) are determined from these feature regions. Further, these control points are modeled geometrically so that the features can be represented with minimum space. A 3D polynomial of degree 3 has been fitted to define a feature from a 3D face and therefore, each feature can be defined by a constant number of coefficients. Instead of storing huge volume of data to define a feature, it is sufficient to store only these coefficients. Finally, these coefficients can be used to identify a 3D face. In case of biometric identification, often there is a need to search a large database for matching which may require substantial amount of response time and hence it is desirable to design some efficient method to reduce the search space. Soft biometric can be used to reduce the search space in the biometric database. For example, the proposed geometric model of each feature from 3D face can be used to classify the database into various classes and this may reduce the search space substantially.

The paper is organized as follows. Next section deals with the overall methodology used for normalization and extracting regions of interest automatically. Section III proposes a method to extract control points or features from each region of interest. Section IV makes use of these control points for 3D face recognition. Experimental results are also analyzed in this section. The next section presents a method of geometric modeling of the extracted features while regeneration method has been discussed in Section VI. Various applications of the proposed model have been presented in the next section and the conclusions are discussed in the last section.

II. REGION OF INTERST EXTRACTION METHODOLOGY

This section proposes new methods to extract regions of interest from the point cloud data of 3D face. Initially the 3D face is normalized to bring it to a standard form. Normalization is done with respect to the entire coordinate axis *X*, *Y* and *Z*; therefore, large pose variations (left tilt/ right tilt and front bent/ backwards bent) can also be handled efficiently. However, it assumes that the face has been scanned from the frontal view and in the scanned face the eyes are in upper half portion of the image. The proposed method makes use of neither intensity information nor texture in order to extract features and therefore, the algorithm is invariant to illumination. It has been tested on BU-3DFE (Binghamton University 3D Facial Expression) Database [16], each having at least 6 expressions. The sample images from the database with different expressions (sad, angry, laughing, neutral, surprised and disgust) are given in Fig.1.

Figure 1. Sample Images in Database with Different Expressions

A. Normalization

A 3D geometric transformation technique has been used to normalize a 3D facial image. It consists of three major steps and they are translation, rotation and scaling. The process of normalization can be initiated by drawing a line joining the points of Z_{max} and Y_{min} which is called ***Face Equator line or FE line.*** This line can be defined mathematically as follows. For a 3D facial image with n points, let us define a 6-tuple $R = \{R_x, R_y, R_z, R_{xn}, R_{yn}, R_{zn}\}$ containing information such as *X, Y* and *Z* coordinates of a point P_i with their corresponding normals X_{Ni}, Y_{Ni}, Z_{Ni}. Let $P_k = (X_k, Y_k, Z_k)$ be a point whose *Z*-coordinate is maximum while $P_l = (X_l, Y_l, Z_l)$ be a point with minimum *Y*-coordinate. On *YZ*-plane, the *FE line* is obtained by drawing line between (Y_k, Z_k) and (Y_l, Z_l) as shown in Fig. 2.

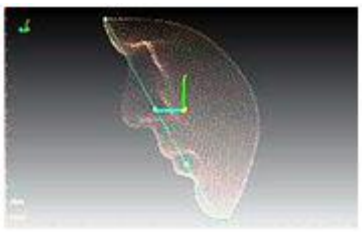

Figure 2. Face Equator Line

There is a possibility that the resultant image may be tilted with respect to *X, Y* and *Z* axes as shown in Fig. 3. To get the frontal face of the image, depending on the tilts in the input image, necessary rotation operation can be performed.

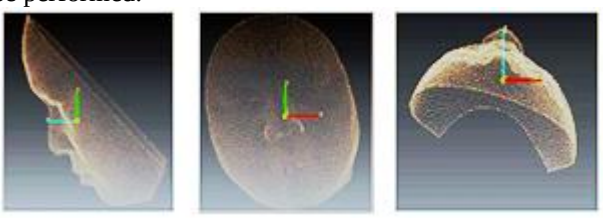

(a) Along *X*-axis (b) Along *Z*-axis (c) Along *Y*-axis

Figure 3. Tilted Face

To eliminate the tilt along *X*-axis, the angle α of *FE line* with *Y*-axis by which the image has to be rotated can be obtained by

$$\alpha = \tan^{-1}[(Y_l - Y_k)/(Z_l - Z_k)]$$

If $\boldsymbol{S_i}$, $\boldsymbol{S_n}$, $\boldsymbol{M_x}$, $\boldsymbol{S'_i}$ and $\boldsymbol{S'_n}$ are location vector, normal vector of original point cloud, 3D rotation matrix with respect to *X*-axis, location vector and normal vector of new point cloud respectively, then the image can be rotated with respect to its positive *X*-axis by an angle α as:

$$\boldsymbol{S}'_i = \boldsymbol{M_x} * \boldsymbol{S_i} \text{ and } \boldsymbol{S'_n} = \boldsymbol{M_x} * \boldsymbol{S_n}$$

where

$$S_i = \begin{pmatrix} X_i \\ Y_i \\ Z_i \\ 1 \end{pmatrix}, S_n = \begin{pmatrix} X_{Ni} \\ Y_{Ni} \\ Z_{Ni} \\ 1 \end{pmatrix}, M_x = \begin{pmatrix} 1 & 0 & 0 & 0 \\ 0 & \cos(\alpha) & -\sin(\alpha) & 0 \\ 0 & \sin(\alpha) & \cos(\alpha) & 0 \\ 0 & 0 & 0 & 1 \end{pmatrix}, S'_i = \begin{pmatrix} X'_{Ni} \\ Y'_{Ni} \\ Z'_{Ni} \\ 1 \end{pmatrix}, S'_n = \begin{pmatrix} X'_{Ni} \\ Y'_{Ni} \\ Z'_{Ni} \\ 1 \end{pmatrix}$$

In the resultant rotated image, the point having the maximum *Z*-coordinate is the nose tip of a human face and is termed as *Lunar Point*. Let the coordinate of the nose tip, *nt*, be (X_{nt}, Y_{nt}, Z_{nt}). The rotated image along *X*-axis of Fig.3 (a) is shown in Fig 4(a).

Given the new point cloud vectors as above, the tilt of the image with respect to *Z*-axis by angle γ which is between *XY* projection of *FE* line and *Y*-axis can be eliminated by

$$\boldsymbol{S}'_i = \boldsymbol{M_z} * \boldsymbol{S_i} \text{ and } \boldsymbol{S'_n} = \boldsymbol{M_z} * \boldsymbol{S_n}$$

where the rotation matrix $\boldsymbol{M_z}$ with respect to *Z*-axis is

$$M_z = \begin{pmatrix} \cos(\gamma) & 0 & -\sin(\gamma) & 0 \\ \sin(\gamma) & 0 & \cos(\gamma) & 0 \\ 0 & 0 & 1 & 0 \\ 0 & 0 & 0 & 1 \end{pmatrix}$$

and S'_i and S'_n are the location vector and normal vector of new point cloud respectively. The rotated image along *Z*-axis of Fig. 3(b) is shown in Fig 4(b).

Consider the case shown in Fig. 3(c) where the face is tilted along *Y*-axis. To eliminate the respective tilt with respect to *Y*-axis, the angle β needs to be computed. This is done first by computing the horizontal curve along the nose tip. Consider the set of points $P_h = \{X_h, Y_h, Z_h\}$ where Y_h-coordinate lies between $Y_{nt} - T_h$ and $Y_{nt} + T_h$ for a threshold T_h. This threshold is chosen in such a way that one gets the entire span of nose area and determines the horizontal curve. End points of the horizontal curve are determined by selecting two minimum values among the set of points $\{P_h\}$ along *XZ*-plane with respect to *X* having sufficient distance between these two minimum points. These two points are nothing but side end points of nose viewing in direction of positive *Y*-axis. Let coordinates of these two points N_l and N_r be (X_l, Y_l, Z_l) and (X_r, Y_r, Z_r) respectively. Now, the angle β between *X*-axis and line joining the points N_l and N_r can be obtained by

$$\beta = tan^{-1}[(Z_r - Z_l)/(X_r - X_l)]$$

and the image can be rotated with respect to positive *Y*-axis by angle β to get

$$S''_l = M_y * S'_l \text{ and } S''_n = M_y * S'_n$$

where

$$M_y = \begin{pmatrix} \cos(-\beta) & 0 & \sin(-\beta) & 0 \\ 0 & 1 & 0 & 0 \\ -\sin(-\beta) & 0 & \cos(-\beta) & 0 \\ 0 & 0 & 0 & 1 \end{pmatrix}$$

The rotated image along *Y*-axis of Fig.3(c) is shown in Fig 4(c).

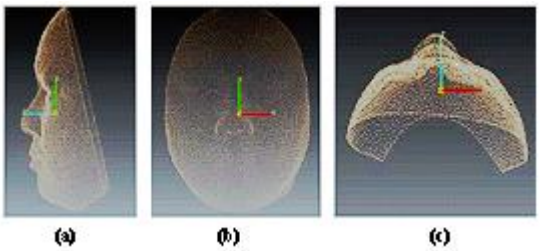

Figure 4. Rotated Images along (a) *X*-axis, (b) *Z*-axis and (c) *Y*-axis

In order to make the standard alignment for feature extraction, the origin is translated to the nose tip having the coordinates (X_{nt}, Y_{nt}, Z_{nt}). Accordingly, coordinates of each point (*X*, *Y*, *Z*) are shifted by $X' = X - X_{nt}$, $Y' = Y - Y_{nt}$, and $Z' = Z - Z_{nt}$ respectively.

Once the nose tip is identified as origin of the image, one can search in the *Y*-direction to determine the depth of a given nose, i.e. nose dip. It can be noted that both nose tip and nose dip lie on the same line. If the *Y*-coordinate of the nose dip is taken as a fixed value, the scaling of faces can be done by taking distance between the nose tip and nose dip along *Y*-axis of the coordinate system. For the 3D face image shown in Fig. 5(a), the corresponding normalized image with nose tip as origin is given in Fig. 5(b).

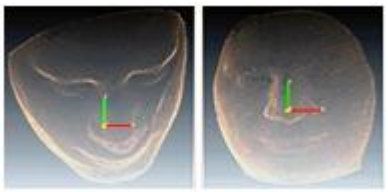

(a) (b)

Figure 5. (a) Original (b) Normalized Image

B. Regions of Interest Extraction Algorithm

The normalized face image has been used to extract the regions of interest such as eyebrows, nose and lips of 3D facial data. It determines the geometry and the shape of the extracted features. The algorithm consists of the following major steps.

Step 1: *(a) Divide the normalized face into uniform rectangular grids;*
(b) Calculate surface normal to each grid;
(c)Determine the regions of interest by computing angle between normal of adjacent horizontal and vertical planes;

Step 2: *Segment the Regions of Interest*

Step 3: *Extract regions like Eyebrow, Nose and Lips*

B.1 Computation of Surface Normals

The feature extraction algorithm mainly computes surface normals. The entire normalized face is divided into 80X72 uniform sizes of rectangular grids as shown in Fig. 6. For each grid, a plane is fitted by the following method. Suppose, X_0 is a point in the given grid which is normal to the unit vector, **n**, in 3- dimensional space. Then for the grid having m points X_i, i =1, 2, ... m, a plane can be described in the following form

$$(X-X_o)^T\mathbf{n} = 0 \text{ with } \|\mathbf{n}\|=1$$

By the method of Orthogonal Distance fitting plane as given in [1], one can define the plane equation of the form aX + bY + cZ + d = 0 for each grid.

Figure 6. Rectangular Grids in Face

The unit surface normal ***n*** for the given plane $aX + bY + cZ + d = 0$ is given by $(a\hat{i} + b\hat{j} + c\hat{k}) / \sqrt{(a^2 + b^2 + c^2)}$. Cosine of angle between the two unit surface normals $A_1\hat{i} + B_1\hat{j} + C_1\hat{k}$ and $A_2\,\hat{i} + B_2\hat{j} + C_2\hat{k}$ of the two adjacent (vertical and horizontal) grids can be obtained by their dot product

$$\cos\theta = a_1*a_2 + b_1*b_2 + c_1*c_2 \qquad (1)$$

Only those adjacent grids whose angles as defined in Eq. 1 are selected to determine the regions of interest. In our experiment, all the adjacent horizontal grids with $\theta \leq 8.89^o$ and all adjacent vertical grids having $\theta \leq 18.19^o$ are considered.

B.2 Region Segmentations

This subsection presents a method to segment regions having the desired features from 3D face. The resultant regions constitute the regions of interest which are used later to extract features like left eyebrow, right eyebrow, nose and lips. From the experiments it has been found that

1. In the eyebrow region, *Y*-coordinate lies between 7.50 and 9.85 while *X*-coordinate is less than 0 for left eyebrow and is greater than 0 for right eyebrow.
2. In the nose region, *X*-coordinate lies between -7.0 and 7.0 while *Y*-coordinate lies between -3.0 and 7.5
3. In the lips region, *X*-coordinate lies between -7.0 and 7.0 while *Y*-coordinate lies between -10.0 and -4.0

Fig.7 shows the segmented regions of a 3D face.

B.3 Region Extraction

Initially, the face is divided into rectangular grids and a plane is fitted on each grid as described in Section B.1. It can be noted that points in an eyebrow can be found out by considering the maximum *Z* value along each vertical column of the grids. Let *j* be the column in the grid. Then the eyebrow region can be defined by the block $B(i,j)$ containing maximum *Z* value for the given column *j*. Fig. 8 shows the extracted eyebrow regions.

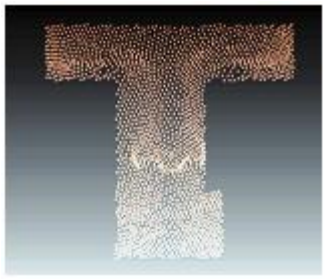

Figure 7. Segmented Region of Face

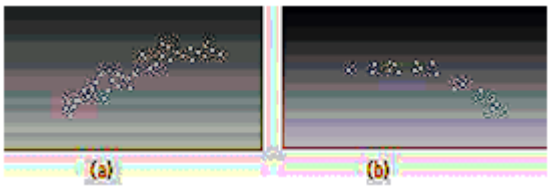

Figure 8. (a) Extracted Left Eyebrow Region (b) Extracted Right Eyebrow Region

For extraction of nose region, horizontal, vertical and angle filtering techniques proposed in [6] can be used. In case of horizontal and vertical filtering, angles between the normals of every pair of adjacent horizontal and vertical planes respectively are found and based on some threshold value, say α, planes are chosen as nose region. This extracted region contains some unwanted portions including cheek region and upper lip region. Angle filtering technique [6] is used to remove these unwanted portions from the extracted region. It can be noted that the normal to the cheek region and the upper lip region may make a very small angle or is almost parallel to *YZ*-plane. Considering this, angle filtering finds an angle, α_{angle}, to eliminate these unwanted portions. Mathematically, horizontal, vertical and angle filtering can be described below.

Let $N(i,j)$ be the normal to the plane at the j^{th} column of the i^{th} row. Let α_1 and α_2 be angles between adjacent horizontal planes and between adjacent vertical planes respectively. Angles α_1 and α_2 can be found by

$$\alpha_1 = \cos^{-1}(N(i,j) * N(i,j+1)) \qquad (2)$$

$$\alpha_2 = \cos^{-1}(N(i,j) * N(i+1,j)) \qquad (3)$$

It has been observed that α_1 lies between 14.07º and 66.42º for adjacent horizontal planes and α_2 lies between 21.57º and 64.53º for adjacent vertical planes.

For angle filtering, we need to compute the angle made between the normal to a plane with *YZ*- plane, α_{angle} which can be obtained by

$$\alpha_{angle} = \cos^{-1}((\mathbf{y}^2 + \mathbf{z}^2)^{1/2}) = \sin^{-1}(\mathbf{x}) \qquad (4)$$

where ***x***, ***y*** and ***z*** are the unit vectors in *X*-, *Y*-, *Z*-directions respectively. Experimentally it has been found that α_{angle} is always more than or equal to 46°. Fig. 9

shows the extracted nose region after applying horizontal, vertical and angle filtering to the nose region.

Figure 9. Extracted Nose Region

For the extraction of lips region, a plane is fitted in the lip region using moment method of orthogonal least square plane fitting [1]. The best fitted plane obtained by this method crosses the lip region in such a way that the maximum lip portion, upper lip and lower lip comes above the plane and rest is below the plane. Thus, the points above the plane are chosen for lip extraction. A plane $F(X,Y,Z)$ can be defined by

$$F(X,Y,Z) = aX + bY + cZ + d \quad (5)$$

All the points that satisfy the following condition are selected as points belonging to lips region

$$F(X,Y,Z) * d > 0$$

This indicates that all these points are above the plane $F(X,Y,Z)$. Fig. 10 shows the extracted lips using the above described method.

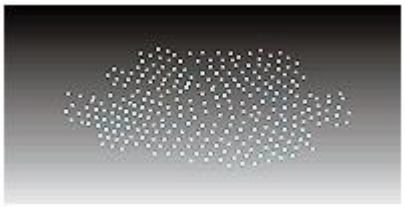

Figure 10. Extracted Lips Region

III. CONTROL POINTS (FEATURES) EXTRACTION

The extracted regions are used to obtain the control points on face. These points represent the minimum set of feature points required to define uniquely a 3D face. The proposed algorithm extracts 12 control points automatically from eyebrows, nose and lip regions. These points are found to be distinct for different faces. The control points are four end points of eyebrows (P_1,P_2,P_3,P_4), two end points of nose (P_5,P_6), nose tip (P_7), nose saddle point (P_8), nose dip(P_9), and end points of lips(P_{10},P_{11}) and centre point of lip line(P_{12}). All these control points are shown in Fig. 11. Given the extracted regions of study, we need to obtain these control points. The process of finding these control points is discussed below.

A. End Points of Left Eyebrow, Right Eyebrow and Nose

Let *PC* be the set of points on left eyebrow and *p, q* be the points that belong to this set and acronyms the first time they *X*-coordinate of points *p* and *q* are represented by *p.X* and *q.X* respectively for the left eyebrow, the control points P_1 and P_2 can be calculated as follows:

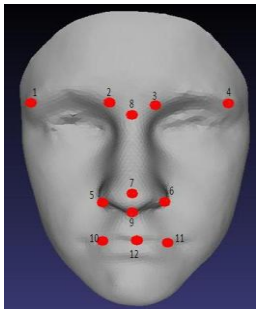

Figure 11. Face Control Points

$$P_1 = \{p \mid p \in PC, q \in PC, p.X \geq q.X, \forall q\} \quad (6)$$

$$P_2 = \{p \mid p \in PC, q \in PC, p.X \leq q.X, \forall q\} \quad (7)$$

Similarly end points P_3 and P_4 of right eyebrow can be computed where in this case, *PC* is a set of points on the right eyebrow. Further, end points P_5 and P_6 of nose can be extracted taking *PC* to be the set of points on nose and similarly end points on lips, P_{10} and P_{11}, can be found by taking *PC* to be the set of points on lips.

B. Nose Tip

This point, P_7, corresponds to the point with maximum *Z*-coordinate value on the face and can be computed as follows:

$$P_7 = \{p \mid p \in PC, q \in PC, p.Z \geq q.Z, \forall q\} \quad (8)$$

where, *PC* is a set of points on face and *p, q* are points in set *PC* and the *Z*-coordinate of points *p* and *q* are represented by *p.Z* and *q.Z* respectively.

C. Nose Saddle Point

Upper most point, P_8, on the nose is termed as the saddle point. It may be noted here that the saddle point has maximum *Z* value between eye pits as we move horizontally and minimum *Z* value as we move down from forehead towards the nose tip. Let $B(i,j)$ represent a grid on i^{th} row and j^{th} column. Now, the problem is to find j_i, for each *i*, such that $B(i, j_i)$ contains maximum *Z* value for row *i*. For this j_i, $B(i, j_i)$ must contain minimum *Z* value in column *j*. Thus, $B(i,j)$ contains saddle point.

D. Nose Dip

This point, P_9, is the minimum *Y*-coordinate just below nose tip in the nose region. Let *NR* be the set of points on nose and *p, q* be the points that belong to this set. The *Y*-coordinate of points *p* and *q* are represented by *p.y* and *q.y* respectively; Then P_9 is given by the following equation.

$$P_9 = \{p \mid p \in NR, q \in NR, -1 \leq p.X \leq 1, p.Y \leq q.Y, \forall q\} \quad (9)$$

E. Lips Mid Point

It is the mid point of lip line. Lip line is the line that divides upper lip and lower lip. Points on this line have minimum *Z* value for each column of grids present in the lip region. Then the lips mid point P_{12} is given by the following equation.

$$P_{12} = \{p \mid p \in LR, q \in LR, -2 \leq p.X \leq 2, p.Z \leq q.Z, \forall q\} \quad (10)$$

where, *LR* is a set of points on face and *p*, *q* are points in set *LR* and the *Z*-coordinate of points *p* and *q* are represented by *p.Z* and *q.Z* respectively.

IV. FACE RECOGNITION

An automatic face recognition attempts to match control points on a given 3D face with the previously stored control points of subjects in a database. All these control points cannot be same for two different faces. Therefore, this technique of matching using control points can give good accuracy. Database is prepared by first calculating the twelve control points for various expressions of a subject as ($P_1, P_2, P_3, P_4, P_5, P_6, P_7, P_8, P_9, P_{10}, P_{11}, P_{12}$) and then storing the average of each control point obtained from various expressions as well as its standard deviation. Thus, one gets twelve control points for each expression of a subject. If the subject has provided images of *m* expressions, then one can determine easily the variations in each control point under each expression. This can be done by taking average and standard deviation of each control point. Let $P_{ij}(k)$ be the j^{th} control point for the i^{th} subject under expression *k*, where, $k = 1$ to 6, $j = 1$ to 12. The average (μ_{ij}) and standard deviation (σ_{ij}) of the j^{th} control point for the subject *i* can be given by

$$\mu_{ij} = \frac{\sum_{k=1}^{m} P_{ij}(k)}{m} \tag{11}$$

$$\sigma_{ij} = \sqrt{\frac{1}{m}\sum_{k=1}^{m}(\mu_{ij} - P_{ij}(k))^2} \tag{12}$$

where $P_{ij}(k)$ is the value of j^{th} control point under k^{th} expression for the subject *i*.

In order to make a decision whether a query subject *Q* matches with the subject *i* in the database, twelve control points P_{ij}, $j = 1,2,\ldots,12$ of the subject *i* are determined using the method discussed in the previous section. Each control point Q_j is compared with P_{ij} of subject *i*. If Q_j is lying between $\mu_{ij} \pm k^*\sigma_{ij}$, for some constant *k*, it is assumed to be matched. Number of such matches is used to take the decision of matching or not matching. Experimentally, *k* is set to the equal error rate (EER) of the test match. The dataset consists of diverse expressions, due to which the standard deviation becomes high and matching results are not very efficient. In laughing expressions, the lower portion around lips may have control points at different positions for the same subject. On calculating the average and standard deviation for all expressions of a subject, it is found that the contribution due to the laughing expression dominates other expressions and reduces the accuracy. If the laughing expression is put into a new bin and the remaining expressions are kept in other bin, then matching based on binning improves the result substantially. Therefore, three bins are formed as (i) one with all expressions (ii) one without laughing (iii) one only with laughing. The query face is sent to appropriate bin for matching based on whether the subject has laughing expression or not.

A. Experimental Results

The proposed algorithm has been tested on BU-3DFE (Binghamton University 3D Facial Expression) database [16] where each subject contains at least six different expressions such as sad, angry, laughing, neutral, surprised, disgust and fear. The correctness of feature extraction is very important to ensure its accuracy. In order to get unique relationship between automatically extracted features and features from original face, a curve is fitted between the end points of respective features and then values on the curve are compared with the original feature values using Chi-Square statistic.

Feature extraction algorithms are found to be accurate with confidence level more than 98.5% for right eyebrow and 99% for other features. The extracted features of the 3D image are shown in Section III. It has been found that these features are well extracted. Table I shows the Chi-Square test results and these results reveals their corresponding confidence levels.

TABLE I
CHI-SQUARE RESULTS

	Test Cases	Confidence Value
Left Eyebrow	228	99.06
Right Eyebrow	228	98.72
Left Nose	228	99.74
Right Nose	228	99.66

The matching algorithm has also used the same BU-3DFE (Binghamton University 3D Facial Expression) database. The results of matching without and with binning are given in Table II and Table III respectively.

TABLE II
MATCHING RESULTS WITHOUT BINNING

	Subjects	Test Images	EER	Accuracy
With Laughing	100	695	4.67	95.33
Without Laughing	100	595	1.27	98.73

TABLE III
MATCHING RESULTS WITH BINNING

	Subjects	Test Images	EER	Accuracy
With Laughing	100	695	1.08	98.92
Without Laughing	100	595	1.27	98.73
Only Laughing	100	100	0	100

In Fig. 12, both FAR and FRR are plotted against various threshold values lying between 1.0 and 3.0. It is found that equal error rate (EER) is 1.08% at the

threshold value of 2.05. In Fig. 13, FRR is plotted against FAR while the graph of GAR against FAR where GAR (Genuine Accept Rate) is calculated as 1 – FRR, is shown in Fig. 14.

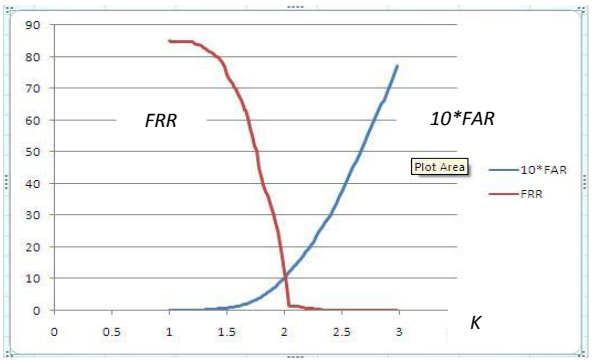

Figure 12. FAR, FRR vs *K*

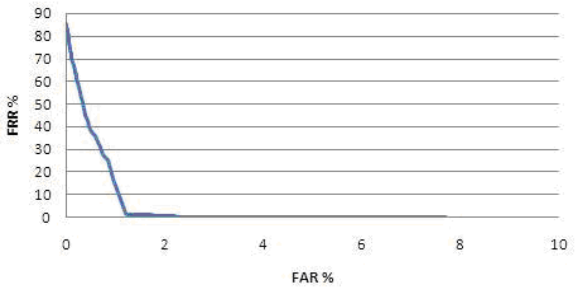

Figure 13. FRR vs FAR Graph

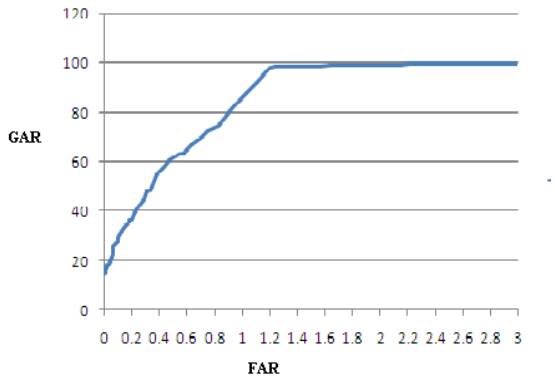

Figure 14. GAR vs FAR Graph

V. GEOMETRIC MODELING OF EXTRACTED FEATURES

Points of each extracted feature are used to fit 2D and 3D curves to define the geometrical model of the feature. Consider a region having n points as (X_1,Y_1,Z_1), (X_2,Y_2,Z_2), (X_3,Y_3,Z_3), …, (X_n,Y_n,Z_n). Also, consider a polynomial of degree 3 to be fitted using the points of an extracted region. Let the 2D polynomial Y and the 3D polynomial Z be of the following form

$$Y = g(X) = A_0+A_1X+A_2X^2+A_3X^3 \quad (13)$$

$$Z = f(x,y) = B_0+ B_1X+ B_2Y+ B_3X^2+ B_4Y^2+ B_5XY+ B_6X^3+ B_7Y^3+ B_8X^2Y+ B_9XY^2 \quad (14)$$

where *A*s and *B*s are constants to be determined by the method of least square. Chi-Square test can be used to determine its goodness of fit.

A. Geometric Modeling of Eyebrows

The extracted points are used to fit a 3D curve in the left and the right eyebrows separately. 2D curve models Y in terms of X for each eyebrow to get coefficients of the model.

B. Geometric Modeling of Nose

Nose is a region of high curvature; two separate curves are used to define regions on nose. The nose is divided into left and right parts about the axis $X = 0$. The two 3D curves are then fitted on the two parts to get coefficients in order to define the nose. The border of nose is defined using 2D curve as left and right curves; X is modeled in terms of Y using the following equation

$$X = g(Y) = A_0 + A_1Y + A_2Y_2 + A_3Y_3 \quad (15)$$

C. Geometric Modeling of Lips

3D curves are fitted on the upper and lower parts to determine their coefficients. A 2D ellipse is fitted on the lips by taking the major axis in X-direction, minor axis in Y-direction and center of the lip line as the center of an ellipse.

D. Geometric Modeling of Face

The face boundary is extracted by finding the maximum and minimum X coefficients on face for Y values in the valid Y range on face. Two separate 3D curves as shown in Eq. 14 are fitted in the left and right boundary of the face. The polynomial coefficients are determined and for each curve along with the range of Y on face, 2D curve models X in terms of Y as given in Eq. 15.

VI. REGENERATION OF FEATURES

This section deals with the problem of regeneration of the face image from the 3D geometric model obtained from the extracted features. Since features are geometrically modeled, in order to regenerate the face, we need to get some control points and the coefficients of the 3D polynomials of degree 3 for various features such as eyebrows, nose and lips. It can be noted that this geometric model of each feature is very useful because it is invariant to scale.

A. Regeneration of Eyebrows

For the regeneration of eyebrows, the coefficients of the polynomials obtained as in Eq. 13 and Eq. 14 and the region belonging to left and right eyebrows are known. Also, there are X_1 and X_2 values corresponding to the minimum and the maximum values of X-coordinate respectively, in the particular region. For different values of X lying between X_1 and X_2, corresponding Y values are estimated using the coefficients obtained in Eq. 13 on the polynomial of degree 3. In the next step, these X and Y values along with the given ten coefficients obtained through Eq. 14 are used to determine the 3D polynomial for the particular feature.

B. Regeneration of Nose

The left part and the right part of the nose are regenerated separately. For each part, points in the nose region such as maximum of Y (Nose Dip), maximum of X

(for the right part of nose) or minimum of X (for the left part of nose) and minimum of Y of the region are given. These points are used to fit three lines to form a triangle. Consider m points (X_i, Y_i, Z) lying in the triangle along Z-axis. These X and Y values along with the given ten coefficients obtained through Eq. 14 are used to determine the 3D polynomial for the nose part.

C. Regeneration of Lips

It requires determining the ellipse equation for the boundary of lips. The maximum and minimum X values and the 3D polynomial of degree 3 for upper and lower lip parts are known. For each X value between the maximum and minimum X on lips, two corresponding Y values are obtained from the ellipse equation and this describes the boundary of the lips. Y values between the obtained maximum and minimum Y along with the corresponding X are put in Eq. 14 for different curves of upper and lower lips separately to obtain the Z-coordinate and regenerate the lip region. The Y values to be put in upper lip and lower lip curves are discretely divided about the middle of lip.

D. Regeneration of Face boundry

The face boundary can be regenerated following the similar procedure described above. The 2D curve obtained in Eq. 15 gives X value of each Y in the complete range of Y on face and Z value for each (X, Y) is obtained from Eq. 14 for left and right side of face respectively.

E. Experimental Results

The proposed algorithm has been tested on BU-3DFE (Binghamton University 3D Facial Expression) database where each subject has various expressions such as sad, angry, laughing, neutral, surprised and disgust. Feature extraction algorithms presented in Section III are found to be accurate with confidence level more than 98% for left eyebrow and 99% for other features. The extracted features of the 3D image given in Fig.5(b) are shown in Fig.15. All these extracted features are combined together to generate the image as shown in Fig. 15(e). It can be seen that these features are well extracted.

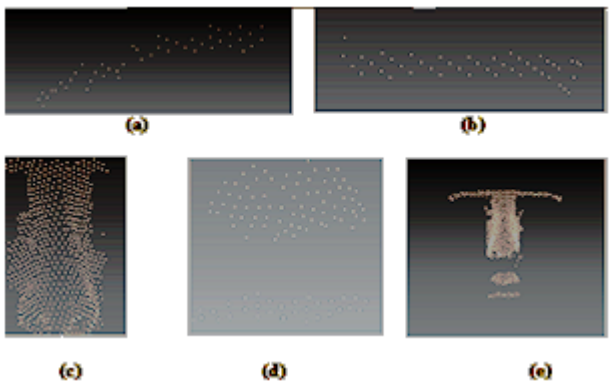

Figure 15. Extracted Features (a) Left Eyebrow, (b) Right Eyebrow (c) Nose (d) Lips and (e) All Combined Features

To the extracted features of the image given in Fig. 15(e), 2D and 3D polynomials of degree 3 using Eq. 13 and Eq. 14 have been fitted and their corresponding coefficients are given in Table IV, Table V and Table VI respectively. Coefficients of ellipse are given in Table VII. Even though the coefficients of degree 3 are very small, its overall effect to the curve is found to be significant.

These coefficients obtained in above tables are used to regenerate the various features of the image given in Fig. 15 (e) and these regenerated features are shown in Fig. 16.

TABLE 1V
COEFFICIENTS ON *XY*- PLANE

Feature (on *XY*-plane)	Left Eyebrow	Right Eyebrow
A_0	47.18900	45.38240
A_1	-0.52070	0.61910
A_2	-0.01540	-0.01680
A_3	-0.00007	0.00009

TABLE V
COEFFICIENTS ON *XY* Z- PLANE

Feature (on *XY*-plane)	Left Nose	Right Nose
A_0	-4.05175	-1.54766
A_1	-0.83723	-0.35037
A_2	0.05315	-0.11358
A_3	-0.11766	-0.02424
A_4	-0.03996	-0.03850
A_5	0.08581	-0.00413
A_6	-0.00178	0.00022
A_7	0.00068	0.00068
A_8	0.00165	-0.00068
A_9	-0.00124	0.00049

TABLE VI
COEFFICIENTS ON *XYZ* -PLANE

Feature (on *XY*-plane)	Upper Lips	Lower Lips
A_0	-270.14800	-341.38272
A_1	-0.43738	-0.20005
A_2	-28.48715	-22.51269
A_3	-0.03933	-0.08842
A_4	-1.04713	-0.51659
A_5	-0.03922	-0.01659
A_6	0.00012	0.00011
A_7	-0.01241	-0.00382
A_8	-0.00038	-0.00151
A_9	-0.00067	-0.00022

TABLE VII
COEFFICIENTS OF ELLIPSE

Coefficients	*Major Axis a*	*Minor Axis b*	*CenterX* C_x	*CenterY* C_y
Ellipse	30.55	6.79	-1.01	-31.17

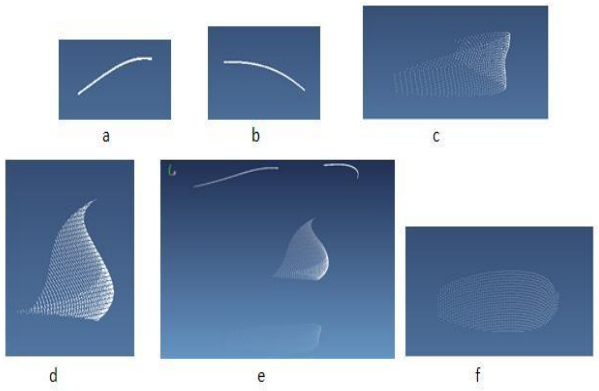

Figure 16. Regenerated Features (a) Left Eyebrow (b) Right Eyebrow (c) Lips Side View (d) Nose (e) All Features (f) Lips Front View

VII. SOME MORE APPLICATIONS

This section discusses some of the applications where these geometric models of the face features can be used. Among the various applications, its use as a soft biometric tool, storage space reduction in the database are worth to mention.

A. Extracted Geometric Model as a Soft Biometric Tool

Biometric traits provide various characteristics based on the behavioral and/ or physiological information about the individual, but lack of the uniqueness and permanence may not be able to differentiate sufficiently between any two individuals. If the general information like gender, age, ethnicity, skin colour, ear shape, geometric features of the face etc. are collected during enrollment, these information can be used as ancillary data to enhance the performance of the system. Jain et. al. [10] have proposed a system where the soft biometric information can be used complimentarily with the primary identity information supplied by the traditional biometric identifiers like fingerprint, face etc. Such auxiliary information can also be used for filtering, by reducing the search zone for a large database, thereby improving the speed and search efficiency of the biometric system. For example, if the shape of the ear is round, the search can be restricted only to the subjects with this profile enrolled in the database.

The proposed geometric models for five features, viz. left eyebrow, right eyebrow, nose, upper lip and lower lip, obtained from *3D* face image can be used to classify the large database into some classes. It can be noted that the geometric model of each feature has been represented by 10 coefficients. Let the class of a *3D* face *F* be denoted by a 5-tuple element $C = [c_1, c_2, c_3, c_4, c_5]$ where c_1, c_2, c_3, c_4 and c_5 are the classes of the left eyebrow, of the right eyebrow, of the nose, of the upper lip and of the lower lip respectively for the given face *F*. In order to determine the class of a given face for a feature *i*, one can follow the following procedure.

Let there be *n* faces belonging to the class c_i with respect to feature *i*. Let us assume that $b_{i1}, b_{i2}, ..., b_{i10}$ are the coefficients attached to the class c_i where b_{ij} is the average of the j^{th} coefficient of *n* faces belonging to the class c_i. Let w_j be the weight assigned to the coefficient b_{ij}. Let $a_1, a_2, ...,a_{10}$ be the coefficients of feature *i* for a given face, then it looks for a class c_i such that $\sqrt{\Sigma_{j\leq 10} w_j (a_j - b_{ij})^2} \leq \varepsilon_i$ where ε_i is the predefined threshold for the class c_i. If m_i is the number of classes of feature *i*, then the total number of classes is $M = \Pi_{i\leq 5} m_i$. Since classes are equally likely, the expected number of faces in each class is *N/M* where *N* is the total number of faces in the database. Let there be *P* faces belonging to the class $C = [c_1, c_2, c_3, c_4, c_5]$. In order to make the search efficiently, these faces are to be indexed in such a way that the number of searches is minimum. There exist several well known multi-dimensional indexing techniques, such as *Range* tree, *kd*-tree, *R**-tree, etc. [17] which can be used to index these *P* faces.

B. Storage Space Reduction

Various features are defined by the 3D polynomial of degree 3 i.e. by some constant number of coefficients. So, instead of storing complete vector for each feature which may contain a large volume of data, the corresponding feature can be represented by storing these coefficients. Through experiment it has been seen that the reduction is more than 90%. Since a 3D face recognition system handles large amount of data, and a large database, so the proposed geometric model for each feature determined from 3D face can be considered to incorporate in the recognition system.

VIII. CONCLUSION

This paper has proposed a method to model various features of 3D faces geometrically. Features which are extracted from the regions of interest like eyebrows, nose and lips are called control points. These control points are further used for 3D face recognition. The method has been tested on BU-3DFE (Binghamton University 3D Facial Expression) Database [16] and its accuracy is 98.92%. From the geometrically defined model an attempt has been made to regenerate all the features such as eyebrows, nose and lips and finally to obtain the whole face. The regenerated method is having accuracy of more than 98% and these faces are found to be invariant to scale, rotation, pose and illumination. Further, this paper has also discussed some other applications of the proposed system.

ACKNOWLEDGEMENT

Authors are thankful to the reviewer for their valuable comments which have substantially improved the quality of the paper. First author also acknowledges Dr. Lijun Yin of Binghampton University who has provided the 3D face database to test the proposed system.

REFERENCES

[1] Ahn S J (2004), Least Squares Orthogonal Distance Fitting of Curves and Surfaces in Space, Springer-Verlag.

[2] Barlett M S, Lades H S, Sejnowski T J (1998) Independent Component Representations for Face Recognition, Proceedings of International Conference on SPIE Human Vision and Electronic Imaging III, Vol. 3299, pp. 528-539.

[3] Belhumeur P N, Hespanha J P, Kriegman D J (1977), Eigenfaces vs. Fisherfaces: Recognition using Class Specific Linear Projection, IEEE Transaction on Pattern Analysis Machine Intelligence, Vol. 19, No. 7, pp. 711-720.

[4] Chang K I, Bowyer K W, Flynn P J (2005), Adaptive Rigid Multi-region Selection for Handling Expression Variation in 3D Face Recognition, Proceedings of IEEE Workshop on Face Recognition Grand Challenge Experiments, San Diego, CA.

[5] Chellappa R, Wilson C, Sirohey S (1995), Human Machine Recognition of Faces: A Survey, Proceedings of IEEE, Vol. 83, No. 5.

[6] Dixit V. K., Singh S., Tiwari H., Goyal S. K., Pathak V. K., Gupta P., Automatic 3D Facial Feature Extraction Algorithm. Proceedings of IEEE International Conference on New Technologies, Mobility and Security, (2008), pages 106-110.

[7] Flynn P J, Faltemier T, Bowyer K W (2008), 3D Face Recognition, in Handbook of Biometrics, editors: Jain AK, Flynn P, Ross AA, Springer, pp. 211-229.

[8] Gokberk B, Salah A, Akarun, L (2005), Rank-based Decision Fusion for 3D Shae-based Face Recognition, Proceedings of International Conference on Audio- and Video-based Biometric Person Authentication, pp. 1019-1028.

[9] Hesher C, Srivastava A, Erlebacher G (2003), A Novel Technique for Face Recognition using Range Imaging, Proceedings of International Symposium on Signal Processing and its Applications, pp. 201-204.

[10] Jain A K, Nandakumar K, Lu X, Park U (2004), Integrating Faces, Fingerprints and Soft Biometric Traits for User Recognition, Proceedings of International Workshop on Biometric Authentication (BioAW), LNCS, Vol. 3087, pages 259-269, Prague, Springer.

[11] Lee Y, Shim J (2004), Curvature based Human Face Recognition using Depth-weighted Hausdorff Distance, Proceedings of International Conference on Image Processing, pp. 1429-1432.

[12] Liu X, Srivastava A, Gallivan K (2004), Optical Linear Representation of Images for Object Recognition, IEEE Transactions on Pattern Analysis and Machine Intelligence, Vol. 26, pp. 662-666.

[13] Lu X, Jain A K (2005), Integrating Range and Texture Information for 3D Face Recognition, Proceedings of 7th IEEE Workshop on Applications of Computer Vision, pp. 155-163.

[14] Lu X, Jain A K (2006), Automatic Feature Extraction for Multiview 3D Face Recognition, Proceedings of International Conference on Automated Face and Gesture Recognition, pp. 266-271.

[15] Lu X, Jain A K (2008), Deformation Modeling for Robust 3D Face Matching, IEEE Transactions on Pattern Analysis and Machine Intelligence, Vol. 30, No. 8, pp. 1346-1357.

[16] Lijun Yin, Xiaozhou W, Yi S, Jun W, Matthew J R (2006), A 3D Facial Expression Database For Facial Behavior Research, Proceedings of 7th IEEE International Conference on Automatic Face and Gesture Recognition, pp. 211 – 216.

[17] Manolopoulos Y (2005), Nearest Neighbor Search: A Database Perspective, Springer USA.

[18] Manly B F J (1994), Multivariate Statistical Methods: A Primer", 2nd edition, Chapman and Hall.

[19] Moreno A, Sanchez A, Velez J, Diaz F (2003), Face Recognition using 3D Surface Extracted Descriptors, Proceedings of International Conference on Irish Machine Vision and Image Processing (IMVIP).

[20] Papatheodorous T, Rueckert D (2005), Evaluation of 3D Face Recognition using Registration and PCA, Proceedings of International Conference on Audio- and Video-based Biometric Person Authentication, pp. 997-1009.

[21] Phillips P J, Moon H, Rizvi S, Rauss P (2000), The FERET Evaluation Methodology for Face-Recognition Algorithms, IEEE Transactions on Pattern Analysis and Machine Intelligence, Vol. 22, pp. 1090-1104.

[22] Phillips P J, Flynn P J, Scruggs T, Bowyer K W, Chang J, Hoffman K, Marques J, Min J, Work W (2005), Overview of the Face Recognition Grand Challenge, Proceedings of IEEE Conference on Computer Vision and Pattern Recognition.

[23] Russ T, Koch M, Little C (2005), A 2D Range Hausdorff Approach for 3D Face Recognition, Proceedings of International Conference on Computer Vision and Pattern Recognition, pp. 1429-1432.

[24] Srivastava A, Liu X, Hesher C (2003), Face Recognition using Optimal Linear Components of Face Images, Journal of Image and Vision Computing, Vol. 24, No. 3, pp. 291-299.

[25] Tsalakanidou F, Malassiotis S, Strintzis M (2004), Integration of 2D and 3D Images for Enhanced Face Authentication, Proceedings of International Conference on Automated Face and Gesture Recognition, pp. 266-271.

[26] Xu C, Wang Y, Tan T, Quan L (2004), Automatic 3D Face Recognition combining Global Geometric Features with Local Shape Variation Information, Proceedings of International Conference on Automated Face and Gesture Recognition, pp. 308-313.

[27] Zhao W, Chellappa R, Rosenfeld A, Phillips P J (2003), Face Recognition: A Literature Survey, ACM Computing Surveys, Vol. 35, No. 4, 2003, pp. 339-458.